Impact of SC-FDMA and Pilots on PAPR and Performance of Power Domain NOMA-UFMC System

Ajit Singh*, K. Krishna Naik† and C.R.S. Kumar‡
*†Dept. of Electronics Engineering, ‡Dept. of Computer Science & Engineering
Defence Institute of Advanced Technology
Pune, India - 411025
Email: *ajit_pee13@diat.ac.in, †krishnanaik@diat.ac.in, ‡suthikshnkumar@diat.ac.in

***Abstract*—Non-Orthogonal Multiple Access (NOMA) is envisioned as promising 5G multiple access technology due to its throughput gain achieved through grouping mobile nodes having substantial difference in channel conditions and capability to serve large number of users simultaneously at same time, frequency, or code, but with different power levels. Furthermore, modifications in OFDM waveform for relaxed synchronization and supporting short burst communications for Internet of Things (IoT) devices has paved the way for Universal Filtered Multi-Carrier (UFMC) waveform. However, a major disadvantage in deployment of Non-Orthogonal UFMC is the high Peak-to-Average-Power-Ratio (PAPR) being comparable to that of OFDMA. As such, additional PAPR reduction techniques are required for reducing the dynamic range of power amplifier deployed in communication system. We take up Power Domain NOMA (PD-NOMA) in which available power is sliced between users and investigate the performance of SC-FDMA for PD-NOMA UFMC systems for PAPR reduction. UFMC is known to provide additional diversity to transmitter in uplink and facilitates relaxed synchronization at the receiver side in downlink scenario. Simulation results show that in flat-fading scenario, BER performance of proposed system is found to be significantly better than OFDM and UFMC. However, BER performance of proposed system in AWGN channel is seen to be traded off as the extent of SC-FDMA precoding increases. Also, increasing pilots per subband leads to increased PAPR with OFDM, UFMC whereas SC-FDMA for PD-NOMA UFMC system shows stagnation and significant comparative reduction in PAPR values.**

Keywords*—NOMA, PAPR, SC-FDMA, Successive Interference Cancellation, Superposition Coding, UFMC

I. Introduction

5G technology is visualizing a rapid evolution in the design of air interface protocols and standards to serve its multi-faceted requirements. As such, 5G is expected to roll out by early 2020 and the frequency allocations for the same will probably be decided in World Radiocommunication Congress (WRC) meeting due in 2019 [1]. Several Non-Orthogonal techniques have been proposed for upcoming 5G radio access to achieve the vision of 5G. Among these, Non-Orthogonal Multiple Access (NOMA) has been a dominant solution to boost fairness and throughput simultaneously providing reliable spectrum access. In OFDMA, spectrum is segmented optimally for different users on the basis of their channel conditions implying that the users closer to Base Station (BS) are allocated more subcarriers and hence enjoy higher throughput while the cell-edge users are allocated lesser subcarriers since they might fail to even access the channel owing to bad channel conditions (e.g. fading, path loss, shadowing). But, in Power-domain NOMA (PD-NOMA), users with lower SINR (LSU) to BS are favored for fairness in spectrum access compared to higher SINR Users (HSU) as 1) they are allocated higher transmit power by BS, and 2) receiver demodulation complexity is lower for LSU. PD-NOMA employs Superposition Coding (SC) and Successive Interference Cancellation (SIC) at the transmitter and receiver respectively [2]. Apart from fairness, the network experiences lower latency since multiple users are being served at the same time.

UFMC is a candidate for 5G technology for providing adaptive and reliable spectrum access to users. We have considered UFMC above other 5G waveforms such as Generalized Frequency Division Multiplexing (GFDM), Filter Bank Multi-Carrier (FBMC), and Filtered OFDM (F-OFDM) because in UFMC, each user can adaptively transmit its data using variable subband size, filter length, and DFT resolution [3]. In addition, filtering reduces out-of-band emission and also provides soft error protection from varying channel conditions since unlike OFDM, UFMC does not utilize Cyclic Prefix (CP), preventing bandwidth wastage [4]. But UFMC possesses high Peak-to-Average-Power-Ratio (PAPR) (comparable to that of OFDMA) which is detrimental to cost-effectiveness and performance of linear amplifiers. Moreover, PAPR reduction is necessary to mitigate interference to LU for underlay CR operation. Variants of Single Carrier-Frequency Division Multiple Access (SC-FDMA) has been utilized for OFDMA for PAPR reduction [5].

NOMA and UFMC both hike the system performance by packing more signals than mandated by orthogonality conditions in power and frequency domain respectively thereby deliberately introducing Inter Symbol Interference (ISI). At the receiver end, interference resolution for NOMA is taken care of by SIC procedure. For UFMC, filter-based equalization and filter length parameters are used for interference mitigation. In [6] and [7], NOMA technique combined with SC-FDMA for uplink scenario is evaluated. SC-FDMA is used for high power efficiency requirements such as uplink and downlink micro/pico BSs. This paper conceptualizes the the combination of the NOMA and UFMC techniques for effectively utilizing both power and frequency domain resources while reducing the PAPR using SC-FDMA. In this paper, we analyze the impact of various SC-FDMA configurations and pilot addition on PAPR and BER performance in PD-NOMA coupled with UFMC technique. Pilots are added as overhead to the subbands and their effect on PAPR and BER performance is studied.

Notations: Vectors/matrices are denoted by bold symbols with/without italic while scalars are denoted by normal letters. $\mathbb{E}(\cdot)$, $(\cdot)^T$ represent expectation, transpose of the matrix and $|\cdot|$ shows absolute value of a vector.

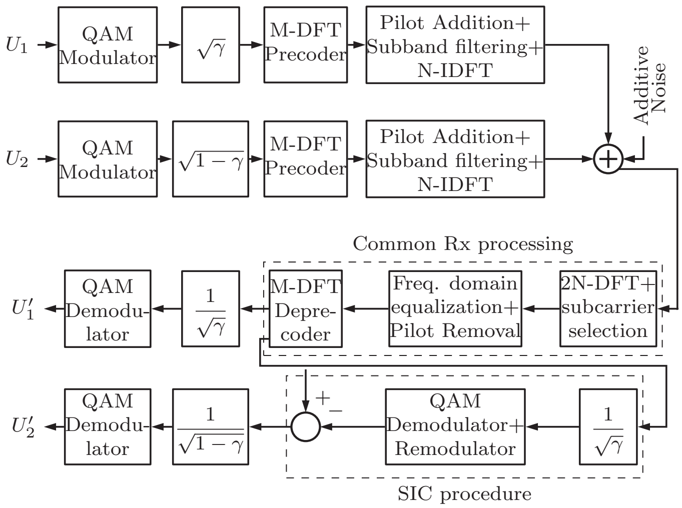

Fig. 1. SC-FDMA in PD-NOMA UFMC network

II. Model Design

PD-NOMA supports both downlink and uplink scenarios where in the downlink, SIC is performed at individual nodes. In the uplink, BS performs SIC for separating users' data from multiplexed signal. However, as noted in [8], if the number of users are increased significantly, the effective performance gain of PD-NOMA over OFDMA saturates while receiver complexity grows in performing SIC. Additionally, if data of even a single user is corrupted, it leads to error-propagation affecting multiple users [9]. A straightforward approach is therefore, to select users with substantial difference in their SINR and pair them for PD-NOMA. In [10], DFT-Spread OFDM with guard interval has been proposed as 5G waveform with only marginal BER leverage compared to OFDM. In our work, however, we have considered SC-FDMA for UFMC with PD-NOMA yielding lower PAPR and significantly improved BER performance. Also, PD-NOMA with UFMC is chosen specifically for relaxing synchronization requirement rather than PD-NOMA with SC-FDMA [6].

Consider typical downlink scenario in which one BS and J mobile nodes are present (refer Fig. 1) [11]. As discussed earlier, we put J=2. BS sends bits $b_l, b_h \in \{0,1\}^{2^{\mathbb{M}} \cdot P}$ for LSU, HSU after which P coded bits $\{c^p_{l,k}\}^P_{p=1}$, $\{c^p_{h,k}\}^P_{p=1}$ are mapped to modulation symbol $d'_l[k], d'_h[k] \in \mathbb{D}$ respectively where $\mathbb{D}$ is a $2^{\mathbb{M}}$-ary QAM constellation set. Resulting P complex symbols are allocated power fractions and multiplexed using Superposition Coding (SC) i.e. $\boldsymbol{d}_l = \sqrt{\gamma} \cdot \boldsymbol{d}'_l$, $\boldsymbol{d}_h = \sqrt{1-\gamma} \cdot \boldsymbol{d}'_h$ and $\boldsymbol{d} = \boldsymbol{d}_l \oplus \boldsymbol{d}_h$ where $\oplus$ refers to Multi User Superposition Transmission Category 1 type technique [12], [13]. Figure 4 illustrates the SC signal constellation identical to that of 16-QAM formed with the superposition of two 4-QAM signals.

Generation of pilots is done using Zadoff-Chu sequence

$$d_{pil}[a] = e^{-j\pi a^2/P_{sub}}, \; a = 0, 1, \cdots, P_{sub} - 1 \qquad (1)$$

which are then slotted in the SC signal at regular intervals on per subband basis. Here, P_{sub} is the total number of pilots. Zadoff-Chu sequences are commonly used for synchronization due to the fact that these sequences exhibit zero autocorrelation when cyclically shifted. Figure 3 shows pilots and UFMC subcarriers stacked together for LSU, HSU and SC signals. Note that Zadoff-Chu sequence is a subset of Constant Amplitude Zero Autocorrelation (CAZAC) sequences (cf. Fig. 4). P complex symbols and P_{sub} pilots are divided into B subbands each comprising of Q subcarriers and C pilots, i.e. $M = (P + P_{sub})/B = Q + C$. Afterwards, each subband data vector $\boldsymbol{d} = \{d[0], \ldots, d[M-1]\}^T$ is precoded using SC-FDMA and spread over N points. At this stage, various Frequency Division Multiple Access (FDMA) schemes for spreading may be applied on the $(M < N)$ symbols. We have employed Distributed FDMA (DFDMA) (DFT data points are placed at regular intervals) and Interleaved FDMA (IFDMA) (interval between DFT data points is such that N/M is an integer) while Localized FDMA (LFDMA) (DFT data points are placed sequentially) is simply inherited when we use only UFMC for transmission [14], [15]. Consider signal $\boldsymbol{D}$ which is obtained after DFT operation as

$$D[k] = \frac{1}{\sqrt{R}} \sum_{m=0}^{M-1} d[m] e^{-j2\pi mk/M}, \;\; 0 \leq k < M \qquad (2)$$

For constructing a signal with oversampling factor $R = N/M$, upsampling by R and an anti-imaging filter is required. Upsampling operation by R and IFFT operation converts the input signal $D[n]$ to $d_u[n] = d[n/R]$ given by

$$d_u[k] = \frac{1}{\sqrt{MR}} \sum_{m=0}^{MR-1} D[k] e^{j2\pi mk/MR}, 0 \leq k < MR \qquad (3)$$

The signal $\boldsymbol{d}_u$ is transmitted via UFMC operation

$$\underset{[(N+L-1)\times 1]}{x_k} = \sum_{i=1}^{B} \underset{[(N+L-1)\times N]}{F_{i,k}} \cdot \underset{[N\times 1]}{d_{u\{i,k\}}} \qquad (4)$$

where for the i^{th} subband ($1 \leq i \leq$ B), d_u symbols are filtered through F which is a Toeplitz matrix performing convolution. Dolph-Chebyshev filter, which is an optimal filter is employed

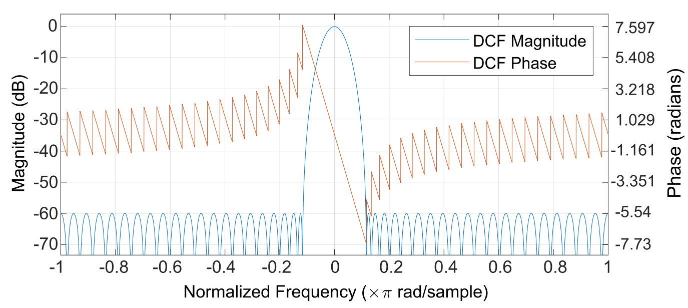

Fig. 2. Magnitude and Phase response of Dolph-Chebyshev filter (L = 43, SLA = 60 dB)

for sub-band filtering in UFMC. For a given filter length L and ripple ratio, Dolph-Chebyshev filter gives minimum possible

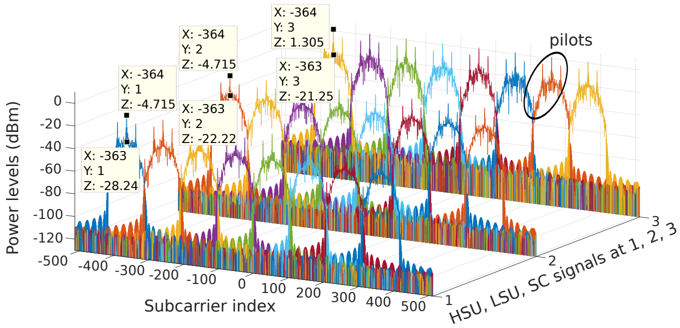

Fig. 3. HSU, LSU and SC signals after UFMC operation with 4 pilots per subband

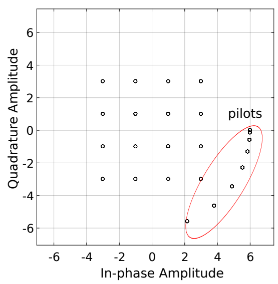

Fig. 4. Arrangement of generated 8 pilots as per Zadoff-Chu Sequence along with 4-QAM LSU, HSU multiplexed signals using SC

main lobe width along with equiripple sidelobes [16]. Frequency domain expression for the DCF window

$$W(k) = (-1)^k \frac{\cos[L\cos^{-1}[\beta\cos(\pi k/L)]]}{\cosh[L\cosh^{-1}\beta]}, \quad 0 \le k \le L-1 \tag{5}$$

$$\text{where} \quad \beta = \cosh[1/L\cosh^{-1}(10^{\alpha})] \tag{6}$$

For calculating Peak-To-Average-Power Ratio (PAPR)

$$PAPR_{dB} = 10\log_{10}\frac{max\left\{\mid x[n]\mid^2\right\}}{\mathbb{E}\left\{\mid x[n]\mid^2\right\}} \tag{7}$$

At the receiver side, $x[k]$, $0 \le k \le N+L-1$ is padded with zeros to extend the samples to $2N$. $2N$-point FFT converts time-domain signal to frequency domain and odd samples are selected. Zero forcing equalization is carried out for estimating symbols at the receiver.

TABLE I. PARAMETERS FOR SIMULATION

Parameter	Values
FFT Points (N_{FFT})	1024
Subband Size (Q)	{16, 14, 12}
Pilots per subband (C)	{0, 2, 4}
Subbands (N_{sub})	16
Filter Length (L)	43
Sidelobe Attenuation (α_{SLA})	60 dB
Frames	100
Oversampling Factor (R)	4
Power Ratio (γ)	0.8
Modulation	4-QAM

III. Results

A. Impact of SC-FDMA and pilots

As mentioned in [8], the performance gain of NOMA over OFDMA is minimal at lower SNR values. Since PAPR varies with block length, we have fixed N_{FFT} = 1024 and modulation scheme as 4-QAM (cf. Table I). BER performance graphs in AWGN scenario indicate that PAPR for PD-NOMA OFDM, UFMC schemes increases with increasing pilots per subband (refer Fig. 5, 7, 9). PAPR values for PD-NOMA IFDMA/DFDMA shows PAPR improvement of max. ∼13.5/10 and min. ∼8/2.5 dB considering all configurations (cf. Table II). However, BER performance of PD-NOMA IFDMA/DFDMA is worse by nearly 7/5 dB at BER=10^{-3} compared to PD-NOMA OFDM/UFMC schemes (cf. Fig. 6, 8, 10). The choice between using IFDMA and DFDMA also depends on required diversity gain and amount of CFO interference [17].

TABLE II. COMPARISON OF PAPR VALUES WITH ODFM AS BASELINE

Scenario	PAPR	
	Absolute (dB)	Relative dB (%)
DFDMA, C=0	8.57	-2.67 (-23.75)
IFDMA, C=0	2.92	-8.32 (-74)
DFDMA, C=2	8.28	-6.16 (-42.66)
IFDMA, C=2	4.56	-9.88 (-68.42)
DFDMA, C=4	7.38	-9.83 (-57.1)
IFDMA, C=4	3.60	-13.61 (-79)

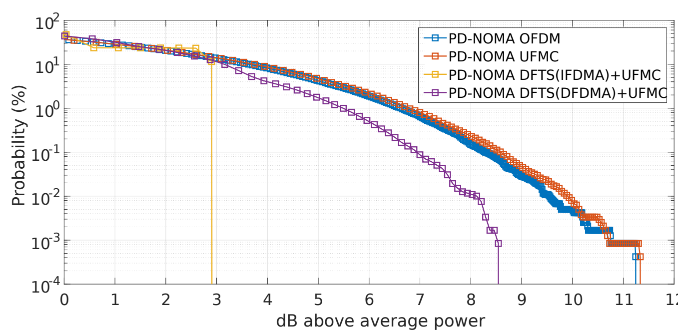

Fig. 5. CCDF of PAPR curves for PD-NOMA (excluding pilots)

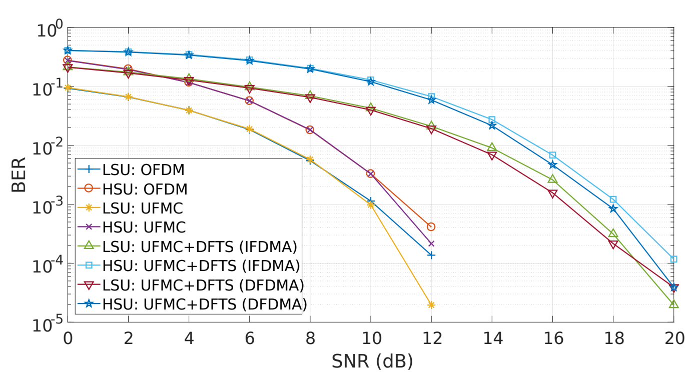

Fig. 6. BER performance curves for various configurations considered for PD-NOMA (excluding pilots)

B. Impact of Rayleigh Flat-fading

In this setting, we consider Rayleigh flat-fading in addition to AWGN channel considered previously. The Channel Impulse

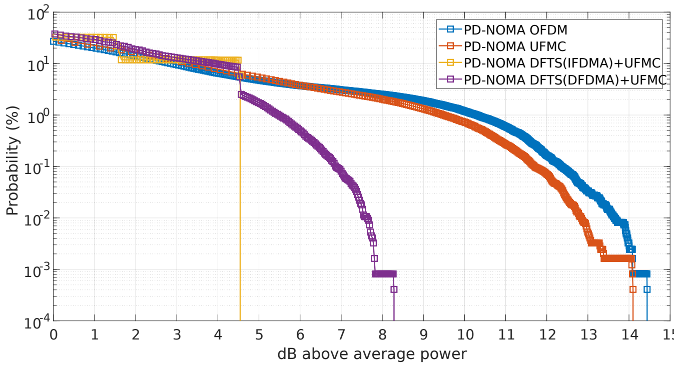

Fig. 7. CCDF of PAPR curves for PD-NOMA (2 pilots per subband)

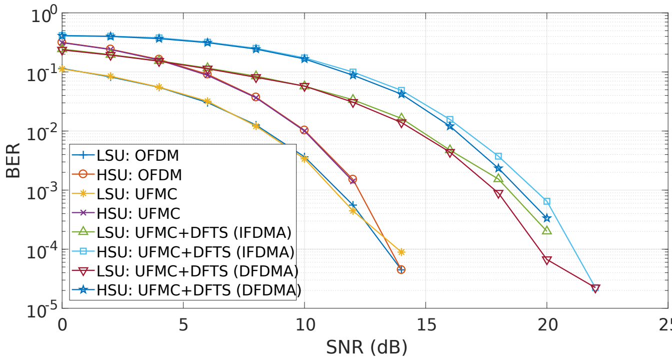

Fig. 8. BER performance curves for various configurations considered for PD-NOMA (2 pilots per subband)

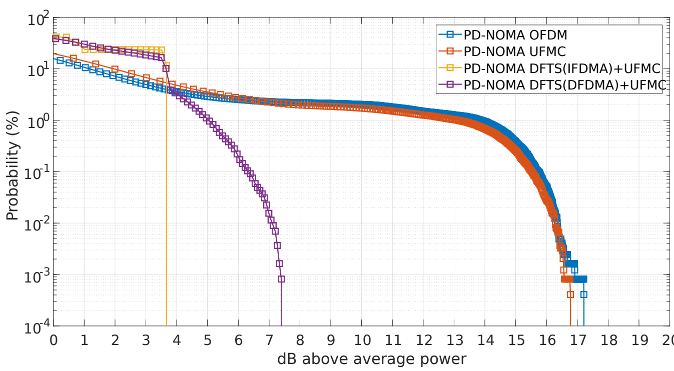

Fig. 9. CCDF of PAPR curves for PD-NOMA (4 pilots per subband)

Response (CIR) for Rayleigh flat-fading channel is given as

$$\boldsymbol{h}_{ray} = \{\mathcal{N}(N_s, 1) + j\mathcal{N}(N_s, 1)\} * \sigma \qquad (8)$$

where $\mathcal{N}(\cdot) \sim$ normal distribution, $N_s = N_{FFT} + L - 1$ is the total number of samples and $\sigma = 1/(\text{SNR} * \text{BPSC})$. In theory, Rayleigh probability distribution function is given by

$$p_R(r) = \frac{r}{\sigma^2} e^{-r^2/2\sigma^2}, \quad r \geq 0 \qquad (9)$$

with r, σ^2 being the magnitude and variance of the distribution. After UFMC operation, the transmit signal $\boldsymbol{x}$ is filtered through Rayleigh flat fading channel as $\boldsymbol{y} = \boldsymbol{x} \cdot \boldsymbol{h}_{ray}$. At the receiver side, we resort to zero forcing method for recovering the faded signal.

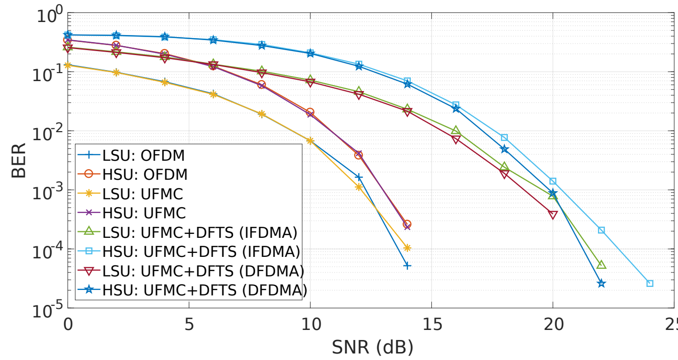

Fig. 10. BER performance curves for various configurations considered for PD-NOMA (4 pilots per subband)

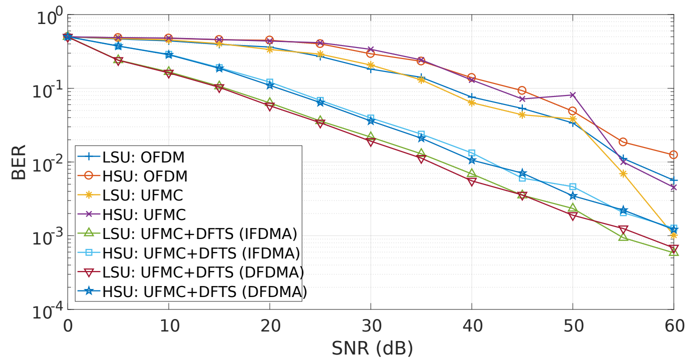

Fig. 11. BER performance curves under Rayleigh flat fading scenario for PD-NOMA configurations

Figure 11 shows the BER performance of various schemes under Rayleigh flat fading channel. Clearly, the proposed SC-FDMA schemes perform better and yield lower BER (cf. Table III). In this case, we have not added any pilots in the system. Additionally, it is observed that at high SNR values, UFMC performs marginally better than OFDM.

TABLE III. COMPARISON OF SNR VALUES FOR AWGN AND RAYLEIGH CHANNELS WITH ODFM AS BASELINE

Scenario	SNR			
	HSU		LSU	
	Absolute (dB)	Relative (dB)	Absolute (dB)	Relative (dB)
AWGN channel (BER=10^{-3})				
DFDMA, C=0	17.92	+6.33	16.83	+6.57
IFDMA, C=0	18.38	+6.80	17.40	+7.13
DFDMA, C=2	19.34	+6.63	17.94	+6.22
IFDMA, C=2	19.77	+7.07	18.81	+7.09
DFDMA, C=4	19.94	+6.36	19.19	+6.39
IFDMA, C=4	20.68	+7.09	19.73	+6.93
Rayleigh flat fading channel (BER=10^{-2})				
DFDMA, C=0	40.86	-19.14	36.12	-19.92
IFDMA, C=0	42.26	-17.73	37.42	-18.63

IV. CONCLUSIONS AND SCOPE FOR FURTHER RESEARCH

We have considered PD-NOMA model with two user groups demarcated as LSU and HSU. In this paper, we have evaluated PD-NOMA UFMC system with SC-FDMA and pilots under AWGN and rayleigh channels. The overhead due to SIC procedure is found to lie in range of 0-5 dB. Results show significant reduction in PAPR while employing SC-FDMA precoding. In Rayleigh flat fading, the proposed scheme performs far better than OFDM/UFMC based PD-NOMA. However, BER performance takes toll when DFDMA is employed and more so on applying IFDMA. The BER performance of PD-NOMA DFDMA/IFDMA at 10^{-3} is nearly 7/5 dB worse than PD-NOMA OFDM while PAPR is better by atleast 8/2.5 dB considering all configurations in AWGN conditions. The BER performance gap for considered SC-FDMA techniques can be minimized using pilot-aided estimation techniques for increased error robustness.

REFERENCES

[1] M. J. Marcus, "Wrc-19 issues: A survey," *IEEE Wireless Commun. Mag.*, vol. 24, no. 1, pp. 2–3, 2017.

[2] D. Tse and P. Viswanath, *Fundamentals of Wireless Communication*. Cambridge University Press, 2005.

[3] G. Wunder, M. Kasparick, T. Wild, F. Schaich *et al.*, "5gnow: Intermediate frame structure and transceiver concepts," in *GC Wkshps*. IEEE, 2014, pp. 565–570.

[4] F. Schaich and T. Wild, "Waveform contenders for 5gofdm vs. fbmc vs. ufmc," in *ISCCSP*. IEEE, 2014, pp. 457–460.

[5] E. E. Tsiropoulou, A. Kapoukakis, and S. Papavassiliou, "Uplink resource allocation in sc-fdma wireless networks: A survey and taxonomy," *Comp. Netw.*, vol. 96, pp. 1–28, 2016.

[6] X. Chen, A. Benjebbour, A. Li, and A. Harada, "Multi-user proportional fair scheduling for uplink non-orthogonal multiple access (noma)," in *Vehicular Technology Conference (VTC Spring), 2014 IEEE 79th*. IEEE, 2014, pp. 1–5.

[7] A. Li, A. Benjebbour, X. Chen, H. Jiang, and H. Kayama, "Uplink non-orthogonal multiple access (noma) with single-carrier frequency division multiple access (sc-fdma) for 5g systems," *IEICE Transactions on Communications*, vol. 98, no. 8, pp. 1426–1435, 2015.

[8] Z. Ding, Z. Yang, P. Fan, and H. V. Poor, "On the performance of non-orthogonal multiple access in 5g systems with randomly deployed users," *IEEE Signal Process. Lett.*, vol. 21, no. 12, pp. 1501–1505, 2014.

[9] S. R. Islam, N. Avazov, O. A. Dobre, and K.-S. Kwak, "Power-domain non-orthogonal multiple access (noma) in 5g systems: Potentials and challenges," *IEEE Commun. Surveys Tuts.*, vol. 19, no. 2, pp. 721–742, 2017.

[10] U. Kumar, C. Ibars, A. Bhorkar, and H. Jung, "A waveform for 5g: Guard interval dft-s-ofdm," in *GC Wkshps*. IEEE, 2015, pp. 1–6.

[11] Y. Wang, B. Ren, S. Sun, S. Kang, and X. Yue, "Analysis of non-orthogonal multiple access for 5g," *China Commun.*, vol. 13, no. Supplement2, pp. 52–66, 2016.

[12] J. M. Meredith, "3gpp technical specification group radio access network - study on downlink multiuser superposition transmission (must) for lte (release 13)," Online Document, 3GPP, Technical Report 36.859, December 2015.

[13] Y. Yuan, Z. Yuan, G. Yu, C.-h. Hwang, P.-k. Liao, A. Li, and K. Takeda, "Non-orthogonal transmission technology in lte evolution," *IEEE Commun. Mag.*, vol. 54, no. 7, pp. 68–74, 2016.

[14] H. G. Myung, "Introduction to single carrier fdma," in *Euro. Sig. Proc. Conf.* IEEE, 2007, pp. 2144–2148.

[15] H. G. Myung, J. Lim, and D. J. Goodman, "Peak-to-average power ratio of single carrier fdma signals with pulse shaping," in *PIMRC*. IEEE, 2006, pp. 1–5.

[16] A. Antoniou, *Digital signal processing: signals, systems and filters*. McGraw-Hill, 2006.

[17] S. Song, G. Chen, and K. B. Letaief, "Localized or interleaved? a tradeoff between diversity and cfo interference in multipath channels," *IEEE Transactions on Wireless Communications*, vol. 10, no. 9, pp. 2829–2834, 2011.